Biosensors and Bioelectronics 38 (2012) 107–113

Contents lists available at SciVerse ScienceDirect

Biosensors and Bioelectronics

journal homepage: www.elsevier.com/locate/bios

Chitosan encapsulated quantum dots platform for leukemia detection

Aditya Sharma [a,b], Chandra Mouli Pandey [a], Gajjala Sumana [a], Udit Soni [b], Sameer Sapra [b], A.K. Srivastava [a], Tathagat Chatterjee [c], Bansi D. Malhotra [a,d,*]

[a] Department of Science & Technology Centre on Biomolecular Electronics, Biomedical Instrumentation Section, Materials Physics & Engineering Division, National Physical Laboratory (Council of Scientific & Industrial Research), Dr K.S. Krishnan Marg, New Delhi 110012, India
[b] Department of Chemistry, Indian Institute of Technology Delhi, New Delhi 110016, India
[c] Department of Pathology, Army Hospital (Research & Referral), Delhi Cantt 110010, India
[d] Department of Biotechnology, Delhi Technological University, Delhi 110042, India

ARTICLE INFO

Article history:
Received 9 February 2012
Received in revised form
26 April 2012
Accepted 8 May 2012
Available online 16 May 2012

Keywords:
Electrophoretic deposition
Nucleic acid hybridization
Quantum dots
Nanocomposite
Chronic myelogenous leukemia
Electrochemical biosensor

ABSTRACT

We report results of the studies relating to electrophoretic deposition of nanostructured composite of chitosan (CS)–cadmium-telluride quantum dots (CdTe-QDs) onto indium-tin-oxide coated glass substrate. The high resolution transmission electron microscopic studies of the nanocomposite reveal molecular level coating of the CdTe-QDs with CS molecules in the colloidal dispersion medium. This novel composite platform has been explored to fabricate an electrochemical DNA biosensor for detection of chronic myelogenous leukemia (CML) by immobilizing amine terminated oligonucleotide probe sequence containing 22 base pairs, identified from BCR–ABL fusion gene. The results of differential pulse voltammetry reveal that this nucleic acid sensor can detect as low as 2.56 pM concentration of complementary target DNA with a response time of 60 s. Further, the response characteristics show that this fabricated bioelectrode has a shelf life of about 6 weeks and can be used for about 5–6 times. The results of experiments conducted using clinical patient samples reveal that this sensor can be used to distinguish CML positive and the negative control samples.

1. Introduction

Chronic myelogenous leukemia (CML) is a hematological disorder caused by t(9;22)(q34;q11) reciprocal translocation of chromosomes 9 and 22, leading to generation of the BCR–ABL oncogene, a protein of 210 kDa (p210BCR–ABL), constitutively active tyrosine kinase. This protein exhibits a disregulated tyrosine kinase activity than the normal ABL protein, leading to activation of several signaling pathways such as Ras/mitogen-activated protein kinase pathway, phosphatidylinositol 3-kinase/Akt pathway and suppression of the mitochondrial pathway of apoptosis, resulting in malignant transformation into CML (Savona and Talpaz, 2008). Since BCR–ABL fusion gene is tumor-specific, early detection of this gene may help in diagnosis of the CML patients by monitoring of the disease after bone marrow transplantation.

The current clinical diagnostic techniques of CML detection include chromosome analysis, fluorescence in situ hybridization, flow cytometry and real-time quantitative reverse transcription PCR. Though, these methods are sensitive for detection of CML, they are time-consuming and hence may result in delay of the treatment. In this context, biosensors have recently attracted much interest in clinical diagnostics due to their high sensitivity, portability and rapid monitoring (Wang, 1999; Pandey et al., 2010, 2011; Sharma et al., 2012). The electrochemical biosensors based on nucleic acid hybridization are being explored for specific detection of CML. Lin et al. (2007) have fabricated an electrochemical DNA biosensor based on glassy carbon electrode (GCE) using methylene blue (MB) as the hybridization indicator. This sensor shows a detection limit of 5.9×10^{-8} M. However, validation with the clinical patient samples has not yet been reported. Chen et al. (2008a) have synthesized 2-nitroacridone (NAD) as the redox label for DNA hybridization. This fabricated sensor exhibits linear response to complementary target DNA with a detection limit of 6.7×10^{-9} M. In another report, these authors have reported a detection limit of 5.3×10^{-9} M using hairpin DNA capture probe and NAD as the electrochemical indicator (Chen et al., 2008b). The attempts have recently been made to improve performance of the biosensor by utilizing locked nucleic acid (LNA) based sequence as the capture probe (Chen et al., 2008c; Wang et al., 2009; Lin et al., 2009, 2010, 2011) that has increased thermal stability when hybridized with its complementary DNA. In spite of these interesting developments, there is an urgent need for the availability of a sensitive, specific and reusable biosensor that can be used for early and reliable detection of CML.

* Corresponding author at: Department of Biotechnology, Delhi Technological University, Delhi 110042, India. Tel.: +91 11 27871043; fax: +91 11 27871023.
E-mail address: bansi.malhotra@gmail.com (B.D. Malhotra).

0956-5663/$ - see front matter © 2012 Elsevier B.V. All rights reserved.
http://dx.doi.org/10.1016/j.bios.2012.05.010

Biomolecular immobilization on a suitable matrix is known to play an important role in the performance of a biosensor. In this context, quantum dots (QDs) have been considered to have great potential for biosensing due to their interesting surface dependent optical properties (Soni and Sapra, 2010), high catalytic efficiency, high surface activity, strong adsorption ability and large specific surface area (Liu et al., 2006, 2007; Li et al., 2009; Martín-Palma et al., 2009; Wu et al., 2010). Recent interest in QDs focuses on their biological applications, not only because of their size dependent properties, but also due to their dimensional similarities with biological molecules resulting in bioconjugates with novel applications (Whaley et al., 2000; Singh et al., 2011). However, Yi et al. (2001) have reported that high surface activity of QDs accompanied with weak interactions with biological molecules may result in agglomeration of QD–bioconjugates. In order to obviate this problem, QDs can perhaps be encapsulated within a polymer matrix that is known to possess reactive functional groups for attachment of the biomolecules. As a functional material, chitosan (CS), a natural cationic polysaccharide, offers unique set of characteristics including hydrophilicity, biocompatibility, biodegradability, chemical stability, non-toxicity and muco-adhesive properties that may be helpful for biomedical applications (Boccaccini et al., 2010). Besides this, surface functionalization of QDs with CS may provide increased affinity towards DNA molecules, owing to the interactions between cationic amino groups on CS and anionic phosphodiester backbone of DNA (Pavinatto et al., 2010).

Among the various techniques used for deposition of nanomaterials and nanocomposites, electrophoretic technique is known to yield uniform, dense and porous films with the advantages of reduced processing time and simple experimental design. In particular, as a wet process, electrophoretic deposition (EPD) provides easy control of thickness and morphology of the deposited film by tailoring various parameters such as deposition time and applied potential etc. (Boccaccini et al., 2010).

In the present manuscript, electrophoretic deposition of CS encapsulated CdTe-QDs (CS–CdTe) is reported for the first time. This CS–CdTe/ITO electrode has been utilized for detection of CML by immobilizing CML specific probe DNA (pDNA) sequence identified from the BCR–ABL gene.

2. Materials and methods

2.1. Chemicals and oligonucleotides

Chitosan (MW: 2.4×10^6 Da), N-ethyl-N-(3-dimethylaminopropyl carbodiimide) (EDC), glutaraldehyde, acetic acid, ethylene diamine tetra acetic acid (EDTA), methylene blue and cadmium perchlorate ($Cd(ClO_4)_2 \cdot 6H_2O$) are of analytical grade and have been obtained from Sigma-Aldrich, India. CML specific probe oligonucleotide sequence (22 bases; UID no. 12859844) identified from BCR–ABL gene of Philadelphia chromosome, complementary, non-complementary and one-base mismatch target sequence, have been procured from Sigma-Aldrich, USA. All the reagents have been prepared in deionized water (Millipore, 18.0 M Ω cm) and the solutions and glassware are autoclaved prior to use. DNA sequences used for the desired studies are as follows:

Probe DNA: Amine–5′–TGTCCACAGCATTCCGCTGACC–3′ (pDNA)
Complementary: 5′–GGTCAGCGGAATGCTGTGGACA–3′
One-base mismatch: 5′–G**C**TCAGCGGAATGCTGTGGACA–3′
Non-complementary: 5′–TACTCGCAATAACGTGATCTCC–3′

These oligonucleotides' solutions are prepared in Tris–EDTA buffer (1 M Tris–HCl, 0.5 M EDTA) of pH 8.0 and stored at −20 °C.

2.2. Processing of clinical patient samples

Extraction of RNA from blood samples of CML positive and negative patients has been accomplished using QIAamp RNA Blood Mini-Kit (QIAGEN). Leukocytes have been separated from lysed blood using selective erythrocytes lysis followed by repetitive homogenizing and washing procedures. The eluted RNA is reverse transcribed to complementary DNA (cDNA) using high-capacity cDNA reverse transcription kit (Applied Biosystems). For this, RT-PCR master-mix is added to RNA and is placed in a thermal cycler, using optimized condition programmed for the kit. The extracted cDNA is diluted 10 times in Tris–EDTA buffer and heated in a water bath (95 °C) for 5 min followed by immediate chilling in ice bath to obtain denatured single-stranded DNA. These aliquots of samples are subjected to sonication at 24 kHz frequency for about 15 min using ultrasonic cleaner, (Vibronics Pvt. Ltd., Mumbai, India) to break long DNA strands into smaller fragments (Sharma et al., 2012).

2.3. Characterization

Ultraviolet–visible (UV–vis) absorption spectra have been recorded using UV–vis spectrophotometer (Phoenix-2200DPCV). Fluorescence emission spectra are collected on a Perkin–Elmer LS-45 spectrophotometer with excitation and emission band widths fixed at 10 nm each. Fourier transform infrared (FT-IR) spectral analysis has been done using Perkin–Elmer, Spectrum BX-II spectrophotometer. The particle size and zeta potential have been determined with a Zetasizer Nano-ZS90 (Malvern Instruments) at a scattering angle of 90° and constant temperature of 25 °C. The morphological characterization has been carried out using a high-resolution transmission electron microscope (HR-TEM, Tecnaii-G2F30 STWIN) and scanning electron microscope (SEM, VP-EVO MA10, Carl Zeiss). The electrochemical characterization has been conducted on an Autolab Potentiostat/Galvanostat (Eco Chemie, Netherlands) using a three-electrode system with ITO coated glass substrate as working electrode, Ag/AgCl as a reference electrode and platinum as a counter electrode, in PBS solution containing 5 mM $[Fe(CN)_6]^{3-/4-}$.

2.4. Preparation of CdTe quantum dots

The synthesis of thioglycolic acid (TGA) capped CdTe-QDs has been done by previously reported method (Gaponik et al., 2002) with slight modification. For this, 0.79 g of $Cd(ClO_4)_2 \cdot 6H_2O$ is dissolved in 100 mL water followed by addition of 0.324 g TGA under continuous stirring. The pH of the solution is adjusted to 12.0 using 1 M NaOH and deaerated by argon bubbling for about 60 min in a three-necked flask. H_2Te gas (generated by the reaction of 100 mg ZnTe powder with 20 mL conc. HCl under Ar atmosphere) is subsequently passed through solution in presence of argon flow, until the solution becomes reddish-brown. The solution is allowed to reflux at 100 °C for about 4 h under open-air conditions. The nanocrystals are washed with acetone and redispersed in water to obtain the concentration of 5 mg/mL.

2.5. Synthesis of CS encapsulated CdTe-QDs

Chitosan solution has been prepared by dissolving 0.05 g of CS in 10 ml of acetic acid solution (0.2 M). CdTe-QDs solution (0.2 ml) is subsequently added to CS solution while stirring, followed by addition of 0.5 mL EDC aqueous solution (0.5% wt/v), which is then left to react overnight at room temperature (27 °C) (Nie et al., 2006). In presence of EDC, the amino groups of chitosan are cross-linked to carboxylic groups on TGA capped CdTe-QDs, leading to formation of the CS–CdTe colloid. This prepared colloidal

solution is centrifuged at 10,000 rpm followed by washing with deionized water thoroughly to remove the free CdTe-QDs. The precipitate is re-dispersed in 50 ml water–ethanol solution (1:4 v/v), by maintaining pH of the solution at about 5.0, to obtain CS–CdTe stock solution.

2.6. Electrophoretic deposition of CS–CdTe onto ITO electrode

Prior to EPD process, ITO coated glass substrates are hydrolyzed by immersing in $H_2O_2/NH_4OH/H_2O$ solution (1:1:5, v/v) for about 30 min at 80 °C. EPD of CS–CdTe composite is carried out with a DC battery (Bio Rad, Model 200/2.0). During the deposition process, 3 ml of CS–CdTe stock solution is diluted with 9 ml of a ethanol which is then cathodically deposited onto hydrolyzed ITO electrode at 10 V for 60 s, using platinum as the counter electrode positioned 20 mm apart. The migration of CS–CdTe colloids towards cathode indicates that these have a net positive charge in solution. This can be attributed to presence of CS on the surface of the nanocomposite that contains primary amino groups with pKa value of around 6.3, below which most of the amino groups get protonated making CS soluble (Jiang et al., 2010; Boccaccini et al., 2010). When voltage is applied between the two electrodes, CS molecules experience a higher pH than pKa near the cathode, wherein amino groups of CS get deprotonated and become insoluble resulting in deposition of the CS–CdTe nanocomposite onto the ITO coated glass substrate (Boccaccini et al., 2010). The plausible mechanism for deposition of the CS–CdTe nanocomposite onto ITO is depicted in Scheme 1. After deposition, the electrode is disconnected from the power supply, removed from the solution, rinsed with Milli-Q water, and stored in a desiccator. For control experiments, CS is also electrophoretically deposited onto ITO coated glass substrate under similar conditions.

2.7. Fabrication of pDNA/CS–CdTe/ITO bioelectrode

Amine terminated probe DNA has been covalently immobilized onto CS–CdTe/ITO electrode using glutaraldehyde as a cross-linker. For this purpose, CS–CdTe/ITO electrode is activated by incubation in an aqueous glutaraldehyde solution (0.1% v/v) for about 4 h followed by washing with deionized water. 20 μL of pDNA (1 μM) is spread onto the electrode surface and incubated overnight for formation of the covalent bond between amine group of pDNA and glutaraldehyde modified CS–CdTe/ITO electrode (Scheme 1). This pDNA/CS–CdTe/ITO bioelectrode is rinsed with Tris–EDTA buffer (pH 8.0) to remove any unbound pDNA from the electrode surface. The prepared pDNA/CS–CdTe/ITO bioelectrode is utilized for CML detection by subjecting it to different concentrations of complementary target DNA for about 30 min and the corresponding difference in current is measured by differential pulse voltammetric (DPV) technique using MB as the redox hybridization indicator.

3. Results and discussion

3.1. Characterization of the quantum dots

The normalized absorption and photoluminescence (PL) spectra of aqueous suspension of CdTe-nanocrystals have been recorded (Supplementary data, Fig. S1). The absorbance maxima at 552 nm corresponding to the first exciton peak (Fig. S1(i)) and fluorescence maxima seen at 564 nm (Fig. S1(ii)) indicate the formation of CdTe-QDs with an average size of 3.2 nm (Yu et al., 2003). The XRD pattern of the crystal (inset, Fig. S1) reveals existence of face-centered cubic CdTe, as indicated by the presence of the characteristic peaks centered at $2\theta = 23.8°$, 39.9° and 46.2°, attributed to (1 1 1), (2 2 0) and (3 1 1), respectively (JCPDS no. 15-0770).

3.2. Characterization of the chitosan encapsulated quantum dots

The particle size distribution and zeta potential of the chitosan encapsulated CdTe quantum dots have been determined via dynamic light scattering. The size distribution profile of the aqueous suspension of CS–CdTe nanocomposite indicates that chitosan encapsulated quantum dots exhibit particle size of ~13–24 nm. Further, the surface charge of the samples has been determined using the Smoluchowski method, and the results are shown in Fig. S2. The TGA capped CdTe-QDs exhibit a zeta potential value of −47 mV (Fig. S2(i)). However, the zeta potential value of QDs after encapsulation within CS polymer has been found to be as +39 mV (Fig. S2(ii)). This reveals the presence of positively charged CS molecules onto CdTe-QDs surface that results in increase of both the particle size and zeta potential. Also, the small particle size of chitosan encapsulated quantum dots and their high zeta potential value indicates stability of this nanocomposite.

3.3. Microscopic analysis of the nanocomposite

The HR-TEM studies have been carried out for morphological investigations of CS–CdTe composite. The uniformly dispersed nanospheres with a diffused contrast reveal encapsulation of the CdTe-QDs within amorphous CS (Fig. S3(i)). Further, appearance of the well-indexed planes at (2 2 0) and (3 1 1), corresponding to fcc crystal structure of CdTe-QDs (Fig. S3(ii)), indicate presence of the original crystal structure of these QDs even after the composite formation with chitosan.

3.4. Spectroscopic analysis of pDNA/CS–CdTe/ITO bioelectrode

FT-IR spectroscopic studies have been carried out to characterize CS–CdTe/ITO electrode and pDNA/CS–CdTe/ITO bioelectrode. The FT-IR spectrum of CS–CdTe/ITO electrode displays peaks at 1642 and 1576 cm^{-1} (Fig. S4(i)), corresponding to amide I and free primary amino group of chitosan at C_2 position of glucosamine along with amide II band. The peaks seen at 1402 cm^{-1} corresponding to C–N deformation, and at 1063 cm^{-1} for –C–O–C– vibration of glucosamine, are attributed to polysaccharide structure of chitosan (Balau et al., 2004). However, in case of the pDNA/CS–CdTe/ITO bioelectrode, the appearance of additional peaks at 1312, 1251, 1152 and 1030 cm^{-1}, corresponding to phosphate stretching, C–O stretching and deoxyribose sugar can be correlated to successful immobilization of probe DNA onto the CS–CdTe/ITO electrode surface (Fig. S4(ii)).

3.5. Morphological characterization of the bioelectrode

The results of morphological studies carried out on CS–CdTe/ITO electrode and pDNA/CS–CdTe/ITO bioelectrode surface are shown in Fig. 1. The uniform morphology has been obtained for CS–CdTe/ITO electrode surface (Fig. 1(i)). However, after incubation of CS–CdTe/ITO electrode with probe DNA, appearance of evenly distributed shiny clusters (Fig. 1(ii)) reveals immobilization of the probe DNA onto CS–CdTe film.

3.6. Electrochemical characterization

The electrochemical studies of CS/ITO electrode, CS–CdTe/ITO electrode, and pDNA/CS–CdTe/ITO bioelectrode have been investigated in phosphate buffer (50 mM, pH 7.0, 0.9% NaCl) containing 5 mM $[Fe(CN)_6]^{3-/4-}$, using cyclic voltammetric technique (Fig. 2).

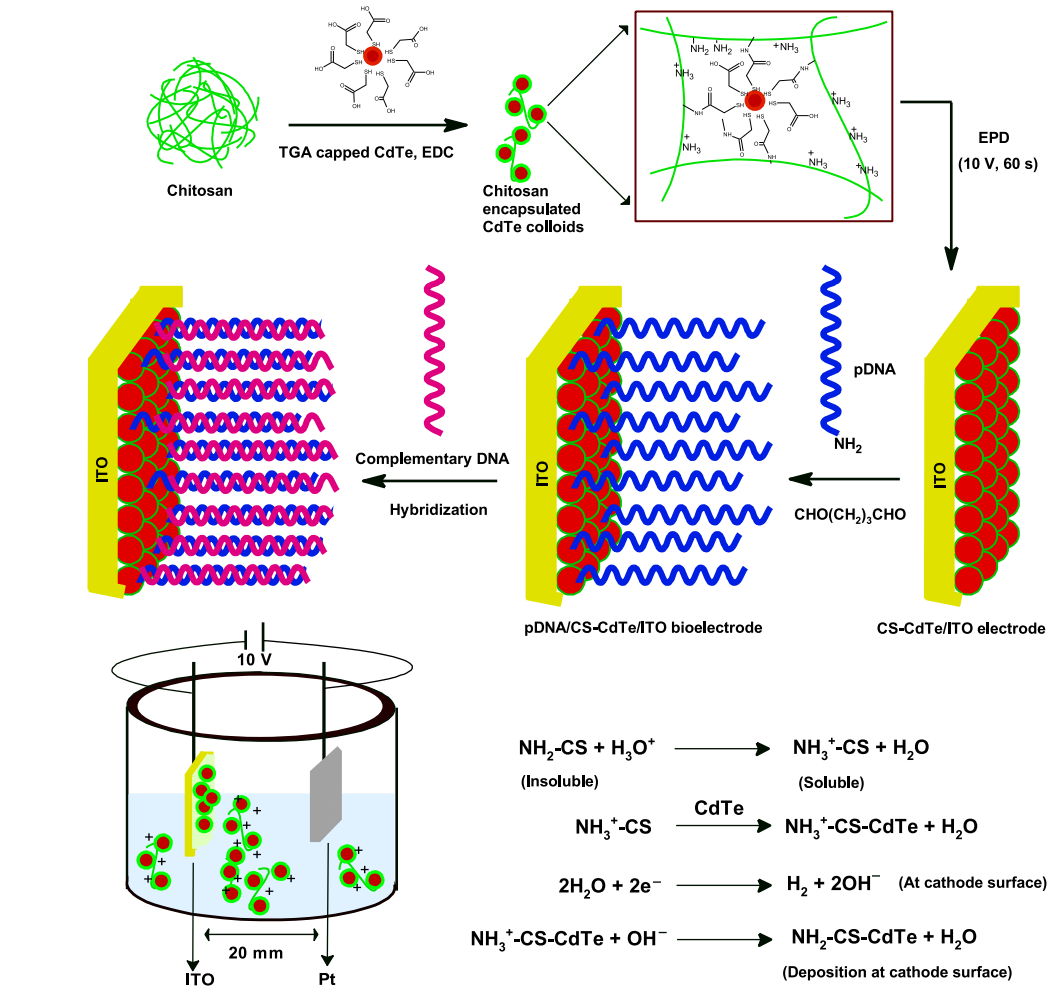

Scheme 1. Schematic showing fabrication of pDNA/CS–CdTe/ITO bioelectrode and the detailed mechanism for EPD of CS–CdTe colloids.

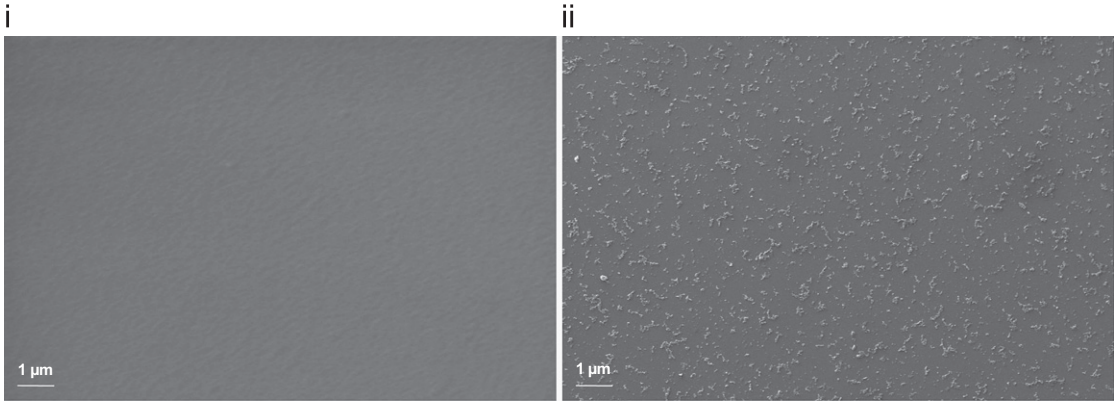

Fig. 1. SEM image of (i) CS–CdTe/ITO electrode and (ii) pDNA/CS–CdTe/ITO bioelectrode.

The cyclic voltammogram of CS/ITO electrode shows sharp redox peaks at 0.48 V and −0.16 V with peak currents of 4.26×10^{-4} A and -3.8×10^{-4} A, respectively (curve (ii)). However, CS–CdTe/ITO electrode exhibits increased peak current (curve (i)) of up to 4.8×10^{-4} A (0.44 V), indicating that CdTe-QDs act as a catalyst to promote electron transfer across the electrode (Lu et al., 2005; Huang et al., 2006; Liu et al., 2006, 2007). On immobilization of pDNA, a sharp decrease in the observed peak current (curve (iii), 3.69×10^{-4} A) with respect to that of the CS–CdTe/ITO electrode is observed. This may be attributed to the sluggish electron transfer across the bioelectrode due to long polymer chain of DNA.

The CV spectra of pDNA/CS–CdTe/ITO bioelectrode recorded as a function of scan rate (10–300 mV/s) are presented (Fig. S5). The anodic and cathodic peak currents (I_{pa} and I_{pc}) exhibit a linear relationship with sweep rate (inset, Fig. S5(i)), suggesting that the

electrochemical reaction is diffusion-controlled (Yang et al., 2006) and follows Eqs. (1) and (2). The peak potential (E_a and E_c) increases as a function of the scan rate (inset, Fig. S5(ii)), indicating facile charge transfer kinetics, and follows Eqs. (3) and (4)

$$I_{pa}\ (\mathrm{A})\ [\mathrm{pDNA/CS{-}CdTe/ITO}] = 2.2926 \times 10^{-4}(\mathrm{A}) + 2.1263 \times 10^{-6}\ \mathrm{A\ (s/mV)}\ [\text{scan rate (mV/s)}];\quad R = 0.9772,\ SD = 4.2861 \times 10^{-5} \tag{1}$$

$$I_{pc}\ (\mathrm{A})\ [\mathrm{pDNA/CS{-}CdTe/ITO}] = -2.3007 \times 10^{-4}(\mathrm{A}) - 1.3906 \times 10^{-6}\ \mathrm{A\ (s/mV)}\ [\text{scanrate(mV/s)}];\quad R = -0.9615,\ SD = 3.6835 \times 10^{-5} \tag{2}$$

$$E_a\ (\mathrm{V})\ [\mathrm{pDNA/CS{-}CdTe/ITO}] = 0.1634\ (\mathrm{V}) + 0.1581\ (\mathrm{V}) * \mathrm{Log}\ [\text{scanrate}];\quad R = 0.9985,\ SD = 0.0037 \tag{3}$$

$$E_c\ (\mathrm{V})\ [\mathrm{pDNA/CS{-}CdTe/ITO}] = 0.1295\ (\mathrm{V}) - 0.1103\ (\mathrm{V}) * \mathrm{Log}\ [\text{scanrate}];\quad R = -0.9754,\ SD = 0.0108 \tag{4}$$

where R and SD are the correlation coefficient and standard deviation, respectively. The diffusion coefficient of the pDNA/CS–CdTe/ITO bioelectrode has been determined using the Randle Sevick equation (Gau et al., 2005):

$$I_p = (2.69 \times 10^5) n^{3/2} A D^{1/2} C v^{1/2} \tag{5}$$

where I_p is the peak current, n is the electron stereochemistry, A is the area of electrode (0.75 cm^2), D is the diffusion coefficient, C is the surface concentration, and v is the scan rate (50 mV/sec). The D value has been obtained to be as 7.7746×10^{-13} cm^2/s. The total surface concentration of pDNA has been calculated using Laviron's theory (Zhuang et al., 2008). The slope is given by following equation:

$$RT/\alpha nF = 0.1581 \tag{6}$$

$$i_p = n^2 F^2 \tau v A (4RT)^{-1} \tag{7}$$

where α represents the transfer coefficient and i_p/v has been calculated from the slope of i_p vs v plot. The total surface concentration of pDNA has been found to be as 2.86×10^{-11} mol cm^{-2} indicating high surface coverage of pDNA onto the CS–CdTe/ITO electrode.

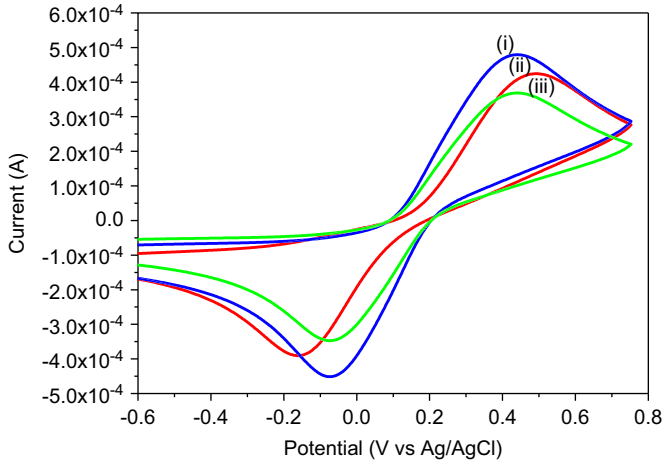

Fig. 2. Cyclic voltammogram of (i) CS–CdTe/ITO electrode, (ii) CS/ITO electrode and (iii) pDNA/CS–CdTe/ITO bioelectrode in PBS (50 mM, pH 7.4, 0.9% NaCl) solution containing 5 mM $[Fe(CN)_6]^{3-/4-}$.

3.7. Electrochemical response studies

Differential pulse voltammetry has been applied to investigate electrochemical response of the fabricated pDNA/CS–CdTe/ITO bioelectrode for detection of CML using MB as a redox hybridization indicator (Fig. 3). Methylene blue is known to undergo reduction by oxidizing the unpaired nucleoside bases of single-stranded probe DNA (pDNA) and it can hence be used to differentiate unhybridized and hybridized DNA (Erdem et al., 2002; Lin et al., 2007). On incubation with the complementary DNA, the MB peak current decreases to ~50% (curve (iv), 1.78 μA) with respect to that of the pDNA/CS–CdTe/ITO bioelectrode (curve (i), 3.30 μA), indicating successful hybridization. It may be noted that negligible change in the peak current (< 10%) is observed for the bioelectrode after incubation with the non-complementary DNA (curve (ii), 3.02 μA) indicating non-hybridization at the pDNA/CS–CdTe/ITO bioelectrode surface. And on incubation with one-base mismatch sequence, significant difference in the peak current (curve (iii), 2.12 μA) is found as compared to that of the complementary sequence indicating partial hybridization. The results obtained with complementary, non-complementary and one-base mismatch indicate selectivity of the fabricated pDNA/CS–CdTe/ITO bioelectrode for CML detection.

The response characteristics of the pDNA/CS–CdTe/ITO bioelectrode have been investigated using DPV by varying target DNA concentration in presence of MB (Fig. 4). It has been found that

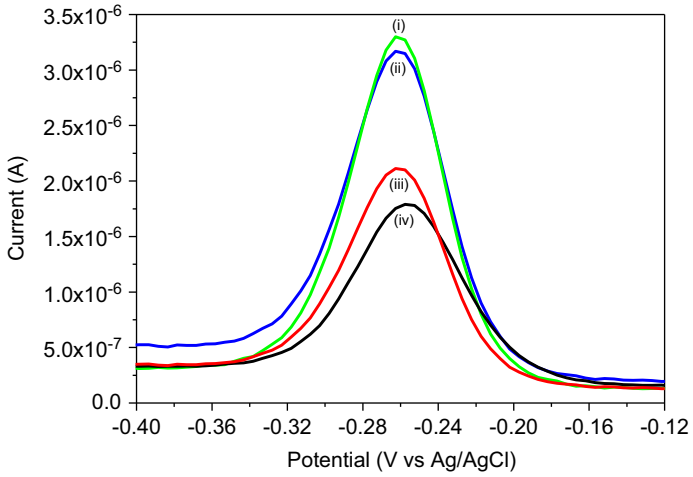

Fig. 3. Differential pulse voltammetric measurements of (i) pDNA/CS–CdTe/ITO bioelectrode with (ii) non-complementary, (iii) one-base mismatch and (iv) complementary target DNA sequence in PBS solution (50 mM, pH 7.4, 0.9% NaCl) containing 20 μM MB.

incubation time of 60 s is sufficient for interaction of MB with the pDNA/CS–CdTe/ITO bioelectrode. The experimental results indicate that the current signal, pertaining to the reduction of MB, decreases with target concentration up to 10^{-6} M and remains constant with further increase in target concentration, revealing that all the immobilized DNA probe molecules on bioelectrode surface participate in the hybridization process at the concentration of 10^{-6} M. The observed reduction current peak, arising due to reduction of MB, is found to be linearly proportional to the concentration of the CML specific target oligonucleotide sequence on the logarithmic scale, in the range from $10^{-6}$to 10^{-11} M (inset, Fig. 4; Eq. (8)).

$$I\,[\text{pDNA/CS–CdTe/ITO}](\text{A}) = 3.3780 \times 10^{-6}(\text{A}) - 2.6942 \times 10^{-7}(\text{A})\,[\log(\text{targetDNAconcentration})] \quad (8)$$

with a standard deviation (*SD*) of 3.6722×10^{-8} and correlation coefficient of -0.9978. The limit of detection, calculated using the expression 3*SD*/sensitivity, is found to be as 2.56 pM. The improved biosensing characteristics have been obtained for this DNA based sensor compared to those reported in literature. This may be attributed to the high charge detaching efficiency of CdTe-QDs that promotes electron transfer from the electrode surface to pDNA molecules.

3.8. Reusability and stability of the bioelectrode

It has been found that the pDNA/CS–CdTe/ITO bioelectrode can be used 5–6 times after regeneration (data not shown). For this purpose, the bioelectrode is immersed in buffer solution (pH 8.0) containing Tris–HCl (10 mM) and EDTA (1 mM) at 100 °C for 5 min, followed by cooling in ice bath for about 30 min, which removes complementary DNA via thermal denaturation (Loaiza et al., 2005). The stability of the bioelectrode is analyzed by measuring response as a function of % reduction in current with respect to time. As shown in Fig. S5, the observed % decrease in the current $<10\%$ up to 46 days indicates stability of the bioelectrode as $\sim$6–7 weeks.

3.9. DPV response of pDNA/CS–CdTe/ITO bioelectrode with clinical patient samples

The specificity of pDNA/CS–CdTe/ITO bioelectrode has been studied with four cDNA samples of each CML positive and negative patients. The observed DPV response indicates significant decrease in the MB reduction current of pDNA/CS–CdTe/ITO bioelectrode on incubation with CML positive patient samples. However, negligible change in peak current is observed with CML negative patient samples (Fig. 5). These results reveal that the fabricated nucleic acid sensor has excellent scope for detection of CML in clinical patient samples. The response characteristics of this pDNA/CS–CdTe/ITO based sensor for CML detection have been compared with those reported in the literature (Supplementary information, Table 1).

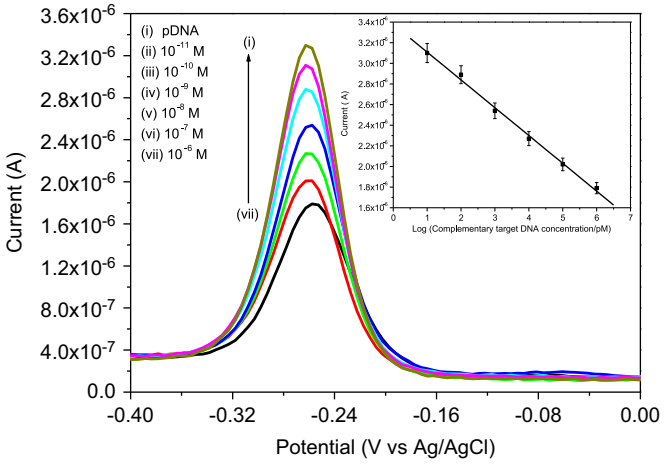

Fig. 4. Sensing characteristics of pDNA/CS–CdTe/ITO bioelectrode as a function of target DNA concentration in PBS solution (50 mM, pH 7.4, 0.9% NaCl) using MB (20 μM) as a hybridization indicator. The inset shows linearity plot for the variation in MB peak height with respect to log of target DNA concentration.

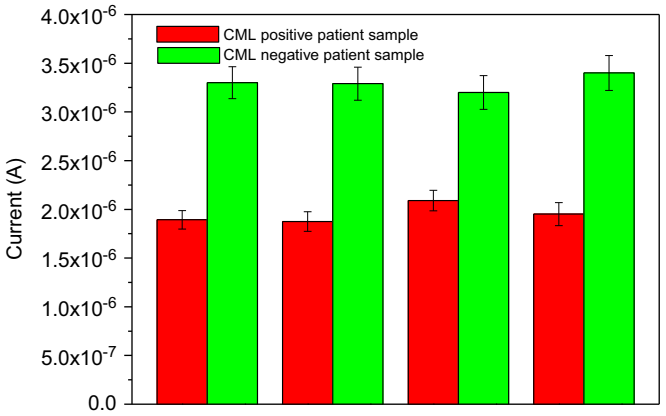

Fig. 5. Histogram showing the DPV response of pDNA/CS–CdTe/ITO bioelectrode as a function of CML positive and negative clinical patient samples.

4. Conclusions

Chitosan encapsulated CdTe-QDs, having positive zeta potential, have been successfully deposited onto ITO coated glass substrates via EPD technique. This nanostructured composite based pDNA/CS–CdTe/ITO bioelectrode is found to detect target DNA in a wide concentration range (10^{-6}–10^{-11} M) with stability of 6–7 weeks, when stored at 4 °C. The fabricated DNA biosensor has been found to distinguish clinical samples of CML positive and negative patients. Efforts should be made to utilize this novel chitosan encapsulated CdTe-QDs electrode to fabricate biosensor with improved detection limit using locked nucleic acid/peptide nucleic acid/micro RNA as the sensing probe.

Acknowledgments

We thank Director, NPL, New Delhi, India for the facilities. AS, CMP and US are thankful to CSIR, India, for the award of Senior Research Fellowship. Thanks are due to Charu Sharma and Sadhana Diwedi for useful discussions and Mr. K.N. Sood (NPL) for SEM measurements. Financial support received under the Department of Science and Technology (DST/TSG/ME/Core-Group/2008) and CSIR (EMPOWER) projects is sincerely acknowledged.

Appendix A. Supporting information

Supplementary data associated with this article can be found in the online version at http://dx.doi.org/10.1016/j.bios.2012.05.010.

References

Balau, L., Lisa, G., Popa, M.I., Tura, V., Melnig, V., 2004. Central European Journal of Chemistry 2, 638–647.
Boccaccini, A.R., Keim, S., Ma, R., Li, Y., Zhitomirsky, I., 2010. Journal of the Royal Society, Interface 7, 581–613.

Chen, J., Zhang, J., Huang, L., Lin, X., Chen, G., 2008a. Biosensors and Bioelectronics 24, 349–355.
Chen, J., Zhang, J., Wang, K., Huang, L., Lin, X., Chen, G., 2008b. Electrochemistry Communications 10, 1448–1451.
Chen, J., Zhang, J., Wang, K., Lin, X., Huang, L., Chen, G., 2008c. Analytical Chemistry 80, 8028–8034.
Erdem, A., Kerman, K., Meric, B., Uzkan, D., Kara, P., Ozsoz, M., 2002. Turkish Journal of Chemistry 26, 851–862.
Gaponik, N., Talapin, D.V., Rogach, A.L., Hoppe, K., Shevchenko, E.V., Kornowski, A., Eychmuller, A., Weller, H., 2002. Journal of Physical Chemistry B 106, 7177–7185.
Gau, V., Ma, S.C., Wang, H., Tsukuda, J., Kibler, J., Haake, D.A., 2005. Methods 37, 73–83.
Huang, Y., Zhang, W., Xiao, H., Li, G., 2006. Biosensors and Bioelectronics 21, 817–821.
Jiang, T., Zhang, Z., Zhou, Y., Liu, Y., Wang, Z., Tong, H., Shen, X., Wang, Y., 2010. Biomacromolecules 11, 1254–1260.
Li, X., Zhou, Y., Zheng, Z., Yue, X., Dai, Z., Liu, S., Tang, Z., 2009. Langmuir 25, 6580–6586.
Lin, X.H., Wu, P., Chen, W., Zhang, Y.F., Xia, X.H., 2007. Talanta 72, 468–472.
Lin, L., Lin, X., Chen, J., Chen, W., He, M., Chen, Y., 2009. Electrochemistry Communications 1, 1650–1653.
Lin, L., Chen, J., Lin, Q., Chen, W., Chen, J., Yao, H., Liu, A., Lin, X., Chen, Y., 2010. Talanta 80, 2113–2119.
Lin, L., Kang, J., Weng, S., Chen, J., Liu, A., Lin, X., Chen, Y., 2011. Sensors and Actuators B 155, 1–7.
Liu, M.H., Shi, G.Y., Zhang, L., Cheng, Y.X., Jin, L.T., 2006. Electrochemistry Communications 8, 305–310.
Liu, Q., Lu, X., Li, J., Yao, X., Li, J.H., 2007. Biosensors and Bioelectronics 22, 3203–3209.
Loaiza, O.A., Campuzano, S., Lopez–Berlanga, M., Pedrero, M., Pingarron, J.M., 2005. Sensors 5, 344–363.
Lu, Q., Hu, S., Pang, D., He, Z., 2005. Chemical Communications 20, 2584–2585.
Martín–Palma, R.J., Manso, M., Torres–Costa, V., 2009. Sensors 9, 5149–5172.
Nie, Q., Tan, W.B., Zhang, Y., 2006. Nanotechnology 17, 140–144.
Pandey, C.M., Singh, R., Sumana, G., Pandey, M.K., Malhotra, B.D., 2010. Sensors and Actuators B 15, 1333–1340.
Pandey, C.M., Sumana, G., Malhotra, B.D., 2011. Biomacromolecules 12, 2925–2932.
Pavinatto, F.J., Caseli, L., Oliveira Jr., O.N., 2010. Biomacromolecules 11, 1897–1908.
Savona, M., Talpaz, M., 2008. Nature Reviews Cancer 8, 341–350.
Sharma, A., Pandey, C.M., Matharu, Z., Soni, U., Sapra, S., Sumana, G., Pandey, M.K., Chatterjee, T., Malhotra, Bansi D., 2012. Analytical Chemistry 84, 3082–3089.
Singh, G., Zaidi, N.H., Soni, U., Gautam, M., Jackeray, R., Singh, H., Sapra, S., 2011. Journal of Nanoscience and Nanotechnology 11, 3834–3842.
Soni, U., Sapra, S., 2010. Journal of Physical Chemistry C 114, 22514–22518.
Wang, J., 1999. Analytical Chemistry 71, 328–332.
Wang, K., Chen, J., Chen, J., Liu, A., Li, G., Luo, H., Lin, X., Chen, Y., 2009. Electroanalysis 21, 1159–1166.
Whaley, S.R., English, D.S., Hu, E.L., Barbara, P.F., Belcher, A.M., 2000. Nature 405, 665–668.
Wu, P., He, Y., Wang, H.F., Yan, X.P., 2010. Analytical Chemistry 82, 1427–1433.
Yang, M., Yang, Y., Yang, H., Shen, G., Yu, R., 2006. Biomaterials 27, 246–255.
Yi, G., Sun, B., Yang, F., Chem, D., 2001. Journal of Materials Chemistry 11, 2928–2929.
Yu, W.W., Qu, L., Guo, Q., Peng, X., 2003. Chemistry of Materials 15, 2854–2860.
Zhuang, Q., Chen, J., Chen, J., Lin, X., 2008. Sensors and Actuators B: Chemical 128, 500–506.